Combining entropy weight and TOPSIS method for selection of tank geometry and filler material of a packed-bed thermal energy storage system

D. Le Roux, Régis Olivès, Pierre Neveu

▶ **To cite this version:**

D. Le Roux, Régis Olivès, Pierre Neveu. Combining entropy weight and TOPSIS method for selection of tank geometry and filler material of a packed-bed thermal energy storage system. Journal of Cleaner Production, 2023, 414, pp.137588. 10.1016/j.jclepro.2023.137588 . hal-04311480

HAL Id: hal-04311480
https://hal.science/hal-04311480v1

Submitted on 28 Nov 2023

HAL is a multi-disciplinary open access archive for the deposit and dissemination of scientific research documents, whether they are published or not. The documents may come from teaching and research institutions in France or abroad, or from public or private research centers.

L'archive ouverte pluridisciplinaire **HAL**, est destinée au dépôt et à la diffusion de documents scientifiques de niveau recherche, publiés ou non, émanant des établissements d'enseignement et de recherche français ou étrangers, des laboratoires publics ou privés.

Distributed under a Creative Commons Attribution - NonCommercial - NoDerivatives 4.0 International License

Combining entropy weight and TOPSIS method for selection of tank geometry and filler material of a packed-bed thermal energy storage system

D. Le Roux[1,2], R. Olives[1,2], P. Neveu[2]*

[1] Procédés, Matériaux et Energie Solaire (PROMES-CNRS), UPR 8521. Rambla de la Thermodynamique, 66100 Perpignan, France

[2] Université de Perpignan Via Domitia, 52 av. P. Alduy, 66100 Perpignan, France

***Corresponding author: dianelerouxgorgodian@gmail.com**

Highlights

- Multi-objective optimisation (exergy, environment and economics) is performed on a thermocline tank.
- Seven different solid filler materials are compared: machined and recycled ceramics or natural rocks.
- TOPSIS method combined with Shannon entropy is used to select the best compromise solution in the Pareto set.
- Ceramics from hard coal ashes were found to be better filler material.

Abstract

Thermocline thermal energy storage systems are promising alternatives for recovering waste heat lost by industry around the world. The aim of this work is to extend the methodology presented in previous work, by optimising an existing industrial packed-bed storage system on two geometric optimisation variables, considering exergy, environmental and economic aspects. Seven filler materials are compared for the same heat transfer fluid, to include discrete variables in the model. The multi-objective optimisation problem is solved using the NSGA-II multi-objective genetic algorithm. For each filler material, a Pareto set is obtained. The non-dominated solutions within the union of the different Pareto sets are then selected, which give a new single set of optimised solutions. A multi-criteria decision-making method (TOPSIS) is then applied to obtain the optimal solution. To avoid any subjective choice from the decision-maker by determining the objective weights of each of the optimisation criteria, the Shannon entropy is used. The combination of TOPSIS and Shannon entropy led to the selection of a recycled ceramic obtained from hard coal ashes as the best filler. This solution has a stocky tank shape (2.4 m diameter, 2.1 m height) and a small particle diameter (7 mm). The exergy and environmental performance is improved compared to the reference storage. They reach 98.0% (vs 95.6%) and 58 hab.year (vs 67 hab.year) respectively. The levelised cost of energy is close to that of the reference tank (3.35 vs 3.31 $c€/kWh_{th}$).

Keywords: waste heat valorisation, life cycle assessment, exergy, life cycle costs analysis, multi-objective optimisation, decision-making methods

1 Introduction

In industry, nearly 50% of the energy consumed worldwide is lost in the form of heat (Forman et al. ,2016). In this sector, 38% of waste heat is at a temperature above 300°C and so requires high temperature solutions for high temperature recovery. In France, this amounts to 10 TWh_{th} lost at over 300°C (ADEME, 2018). A preliminary analysis of the European waste heat field shows that it amounts to 370.41 TWh_{th} per year in industry (Panayiotou et al., 2017). In the US industrial sector, 75 TWh_{th}/year is lost at 150°C (Johnson et al., 2008). In total, the US Department of Energy and the French Energy

Agency (*Agence de l'environnement et de la maîtrise de l'énergie* (ADEME)) estimate that 4,000 to 15,000 TWh_{th} per year could already be recovered worldwide (Plisson et al., 2017). For the deployment of efficient and energy-saving industrial systems, the use of storage devices, particularly thermal, is becoming a necessity. Indeed, these systems can store excess heat rejected by industries into the environment and release it later for delayed electricity or heat generation (Rahman et al., 2020) and thus, would limit energy consumption and greenhouse gas emissions.

In this context, thermocline thermal storage has the potential to improve the energy efficiency of industrial processes. This sensible heat storage uses a single tank inside which the cold and hot fluids reside simultaneously. Compare to two-tank storage, space consumption can decrease by combining the two tanks into one (Fasquelle et al., 2018; Heath et al., 2010), and cost of the system can be reduced down to 35% (Brosseau et al., 2005). In a packed-bed TES, Heat Transfer Fluid (HTF) flows through a Thermal Energy Storage Material (TESM). During the charging step, cold fluid is extracted from the bottom of the tank and hot fluid is injected at the top. As a result, two quasi-isothermal zones (a hot one and a cold one) are separated by a large temperature gradient, called the thermocline zone. During the discharging step, the direction of the HTF is reversed.

Due of the energy and ecological transition, the challenge lies in the implementation and operation of technically efficient systems, verifying a viable and environmentally friendly business model. In view of these different aspects, it is important to optimise TES on several criteria. For this purpose, a multi-criteria optimisation should be performed. The use of multi-objective optimisation methods leads to a set of efficient solutions, called the Pareto set. The points in this set are not dominated by any other, i.e. one or more of the criteria is optimised (minimised or maximised) for these solutions. Multi-objective optimisation methods can be grouped into two main families:

- Deterministic methods transform a multi-objective problem into a single-objective one. Exact algorithms and specific heuristics are part of it,
- Stochastic methods randomly explore the solutions space using probability transition rules. Among them are metaheuristic methods, including evolutionary algorithms consisting of genetic algorithms and particle swarm optimisation.

Stochastic algorithms solve difficult optimisation problems and are easy to implement. They approach the global optimum very quickly. Genetic algorithms are widely used for optimising energy systems that often involve a large number of degrees of freedom: commercial supermarket CO_2 refrigeration system (Dai et al., 2022), PV-Diesel hybrid system for power production in remote area (Tsuanyo et al., 2015), industrial robots in manufacturing industry (Zhang and Yan, 2021), TES tank in cogeneration systems (Wang et al., 2021). Genetic algorithms have been extended for solving multi-criteria optimisation problem. The Non-Dominated Genetic Algorithm (NSGA-II) (Deb et al., 2002) was employed to solve bi-optimisation problems on heavy-duty vehicles (environmental impacts and total cost of ownership through the life cycle eco-efficiency) (Wolff et al., 2021), on noise barrier tunnel (CO2 emissions and costs) (Kim and Kim, 2021), and on combined cooling and power generation system using geothermal system (exergoeconomics) (Ding et al., 2021).

When the multi-objective algorithm is completed, a set of undominated solutions (Pareto front) is obtained. As the solutions in this set are close to each other, it is difficult to choose a solution that outperforms all others, and to rank them unquestionably from best to worst (Hwang and Yoon, 1981). Multi-criteria decision-making methods aim to select a single solution within the Pareto set, and to help decision-makers make a final decision. There are many decision-making methods: TOPSIS (Technique for Order of Preference by Similarity to Ideal Solution) (Hwang and Yoon, 1981), VIKOR (Vlse Kriterijumska Optimizacija I Kompromisno Resenje) (Opricovic, 1998), ELECTRE (*Elimination Et*

Choix Traduisant la REalité) (Maystre et al., 1994), PROMETHEE (Preference Ranking Organisation Method for Enrichment Evaluation) (Brans and Vincke, 1984), AHP (Analytical Hierarchical Program) (Saaty, 1980), LINMAP (Linear Programming Technique for Multidimensional Analysis) (Srinivasan and Shocker, 1973), SECA (Simultaneous Evaluation of Criteria and Alternatives) (Keshavarz-Ghorabaee et al., 2018), fuzzy methods (Zadeh, 1965, 1968)… TOPSIS method is one of the most used in the energy sector (Siksnelyte et al., 2018). This method ranks the Pareto solutions according to their priority. It selects the best compromise solution with the shortest Euclidian distance to the ideal solution and the farthest Euclidian distance to the nadir solution (Hwang and Yoon, 1981).

However, in most multi-criteria decision-making methods such as TOPSIS, a weight is assigned to each criterion, usually subjectively. Decision-makers rank the criteria according to their importance and depending on the subjective weighting method used, the weights are determined. The weight allocation can be influenced by decision-makers' preference. This subjective choice may provide a different solution depending on the weights chosen by decision maker, as observed in sensitivity analysis (Li et al., 2013; Olson, 2004). In order to improve the measurement of uncertainty in the allocation of weights, it is essential to eliminate the influence of subjective factors. In the objective weighting methods, criteria weights are determined by mathematical models, without any consideration of decision-makers. For this purpose, various methods have been developed : Shannon entropy (Huang 2008), standard deviation (Deng, Yeh, and Willis 2000), mean weight (Deng et al. 2000), CRiteria Importance Through Intercriteria Correlation (CRITIC) (Diakoulaki et al., 1995), centralised weights (Solymosi and Dombi, 1986), statistical variance procedure (Rao and Patel 2010). Shannon entropy is one of the most used methods for determining weights in an objective way (Deng et al., 2000; Jing et al., 2018; H.-C. Liu et al., 2019a; X. Liu et al., 2019b; Zhao et al., 2020). This method quantifies the uncertainties of the information source, through a discrete probability distribution (Shannon, 1948). The standard deviation method uses the standard deviations of the criteria to determine their weights. The mean weight considers all criteria to be of equal importance. The CRITIC method is based on the standard deviation to which a linear correlation is applied. The centralised weights method uses centralised distribution to assign weights to each criterion. The closer the solutions are to each other for a criterion, the higher the weight of that criterion relative to the others. The statistical variance procedure uses statistical variance of information. Hybrid methods can also be employed. These methods employ the subjective preference of a decision-maker and apply mathematical models to determine weights. For example, Dos Santos *et al.* (dos Santos et al., 2019) used a hybrid Entropy-TOPSIS with fuzzy sets. The fuzzy approach is combined with Shannon entropy to determine the best green supplier for the Brazilian furniture industry. Saeidi *et al.* (Saeidi et al., 2022) proposed to combine SWARA and Pythagorean fuzzy sets to rank the criteria before applying TOPSIS to find the best sustainable human resource management in factories in Ecuador. Tu *et al.* (Tu et al., 2021) performed a hybrid method integrating hesitant fuzzy linguistic term sets and, decision-making trial and evaluation laboratory (DEMATEL) to determine weights. VIKOR method is then applied to rank the regional coordination of water resources in North China.

In a previous paper (Le Roux et al., 2022b), the importance of combining exergy, environmental and economic aspects was demonstrated to create eco-designed systems. The geometry of an industrial high-temperature thermocline TES, named Eco-Stock®, was successfully optimised according to its exergy efficiency, environmental footprint and cost. However, the optimisation and selection procedures were restricted to a single filler material. This study aimed to extend this primary work for several filler materials. In addition, the methodology developed was using the TOPSIS method with subjective weights, considered equal to each other. As explained above, the choice of criteria weights is crucial in multi-criteria decision-making methods. To avoid expert opinion and improve the decision-

making process, objective weights should be employed. This will be done by weighting the three criteria according to their Shannon entropy. Therefore, the objectives of this study are threefold:

- to compare seven TESM: two machined ceramics (MC), three ceramics obtained from waste, and two natural rocks, Through these objectives, the tri-criteria optimisation performed in (Le Roux et al., 2022b) is improved through the use of Shannon entropy and the comparison of alternative filler materials.
- to improve the optimisation process by building a single Pareto front encompassing several filler materials,
- to improve the decision-making process, by using non-subjective weights based on Shannon entropy.

The article is organised as follows. In the first part (section 2), the description of the system is presented. The methodology developed in (Le Roux et al., 2022b) is briefly outlined and then extended to several filler materials. The decision-making process is also improved through the weighting process based on Shannon entropy. The overall structure of the optimisation problem is finally given. The results are analysed in the third part (section 3). Multi-criteria optimisations are analysed, and the best tank geometry and filler material are simultaneously selected. Then, the trade-off configuration is compared to the reference industrial thermocline storage. The last part concludes (section 4).

2 Material and method

2.1 Problem definition

A three-objective optimisation of an existing industrial high-temperature thermocline tank, called Eco-Stock® (Touzo et al., 2020), is carried out. This storage, developed and commercialised by Eco-Tech Ceram (Eco-Tech Ceram, 2023), recovers waste up to 600°C with an air/bauxite packed-bed and stores $1567\ kWh_{th}/cycle$. Its specifications are reported in Table 1.

Table 1: Specifications of the industrial thermocline tank Eco-Stock®

Design parameters of the tank	**Values**	**Geometric parameters**	**Values**
Maximum theoretical energy capacity Q_{th}	10^{10} J	External shape factor $F_e = D_t/L_t$	0.6228
Porosity ε	40%		
Targeted charging or discharging time t_c or t_{ds}	7.05 hours		
Operating temperatures: hot T_H and low T_L	600 and 20°C	Internal shape factor $F_i = D_s/D_t$	0.0156
Fluid (HTF)	Air		
Solid (TESM)	Bauxite		

This work aims to find the best tank geometry, the best particle size and the best TESM of this industrial thermocline TES according to three criteria: maximising exergy efficiency, minimising environmental impacts and minimising Levelised Cost Of Energy (LCOE).

One of the objectives is to compare seven filler materials appearing interesting for an energy storage application: two commonly used machined ceramics (MC) (bauxite and alumina), three ceramics obtained from waste (ceramics from fly ashes (CFA), ceramics from hard coal ashes (CHCA) and cofalit), and two natural rocks (basalt and quartzite). The thermophysical properties, ecological footprint and costs of each filler are presented in Table 2 at the average operating temperature (310°C). The effusivity ($\epsilon = \sqrt{\lambda \cdot \rho \cdot c}$), which characterises the rate at which a material can absorb heat, was determined. Despite better effusivities, the cost of MC was 30 to 53 times higher than that of recycled

ceramics or natural rocks. The environmental impact of these fillers was 85% and 100% greater than that of ceramics from waste and natural rocks respectively. Therefore, the environmental footprint and cost of the TES device could be lower for fillers derived from waste or natural rocks than for MC.

This question motivated this research is aiming to select the best geometry of the TES tank associated to the best filler material among the seven presented in Table 2.

Table 2: Thermophysical properties (at 310°C), environmental footprint per ton and costs per ton of filler materials

Properties	**Thermophysical properties**				**Environmental impact**	**Cost**
	ρ_s (kg.m^{-3})	c_s (J.kg^{-1}.K^{-1})	λ_s (W.m^{-1}.K^{-1})	ϵ_s (kJ.m^{-2}.K^{-1}.s$^{-1/2}$)	LCA$_s$ (ca.year.ton^{-1})	C_s (€.kg^{-1})
MC – Bauxite	3005	1076	4.0	3.59	0.92	0.9
MC – Alumina	3670	1023	21.0	8.88	0.95	1.6
Recycled ceramic – CFA	2600	1000	1.8	2.16	0.12	0.03
Recycled ceramic – CHCA	2200	1050	1.0	1.52	0.12	0.03
Recycled ceramic – Cofalit	3120	1025	1.8	2.37	0.23	0.03
Natural rock – Basalt	2900	900	2.0	2.29	0.01	0.03
Natural rock – Quartzite	2500	830	5.7	3.44	0.00	0.03

2.2 Multi-criteria optimisation: single filler material case

Modelling and optimisation procedures have been detailed in (Le Roux et al., 2021; Le Roux et al., 2022b) for a single material. They are shortly reminded in this sub-section.

2.2.1 Physical model

The dynamic model consists of solving the transient mass, energy and entropy balances applied to a representative elementary volume, composed of fluid and solid (Rebouillat et al.,2019). It is a one-dimensional (radial gradients are neglected) two-phase model. It models separately the HTF (eq (1)) and the filler material (eq (2)).

$$\varepsilon.(\rho.c)_f.\left(\frac{\partial T_f}{\partial t}+u.\frac{\partial T_f}{\partial z}\right)=\frac{\partial}{\partial z}.\left(\lambda_{eff,f}.\frac{\partial T_f}{\partial z}\right)+h.a_{sf}.(T_s-T_f)+U.a_{fw}.(T_\infty-T_f) \quad (1)$$

$$(1-\varepsilon).(\rho.c)_s.\frac{\partial T_s}{\partial t}=\frac{\partial}{\partial z}.\left(\lambda_{eff,s}.\frac{\partial T_s}{\partial z}\right)+h.a_{sf}.(T_f-T_s) \quad (2)$$

With a_{sf}: specific area between solid and fluid (m^2.m^{-3}), a_{fw}: specific area between fluid and external wall (m^2.m^{-3}), c : heat capacity (J.kg^{-1}.K^{-1}), h: heat transfer coefficient (W.K^{-1}), u: interstitial velocity of the fluid (m.s^{-1}), and U: overall heat loss coefficient between the fluid and the outside (W.m^{-2}.K^{-1}). The subscripts f and s denote respectively the fluid and the solid phases. The thermophysical properties of fluid and solid, assumed constant, are evaluated at the average operating temperature.

The boundary conditions are an imposed temperature at the fluid inlet. A zero second derivative condition is applied to the temperature at the tank outlet for the fluid and the solid. These equations are discretised by a first order centred formulation in space and first order discretisation in time.

The physical model computes the exergy efficiency of the TES. This indicator compares the thermal exergy extracted from the TES by the HTF during the discharging step and the thermal exergy supplied to the TES by the HTF during the charging step.

$$\eta_{ex} = \frac{-\int_0^{t_{ds}} \dot{m} \cdot \Delta ex \cdot dt}{\int_0^{t_c} \dot{m} \cdot \Delta ex \cdot dt} \quad (3)$$

Where t_{ds} and t_c are respectively the duration of the discharging and charging processes, $\dot{m}$ the HTF mass flow rate and Δex the specific exergy changes experienced by the HTF when passing through the storage tank, considering temperature change and pressure drop.

For a given HTF/TESM pair, this model evaluates the energy behaviour and performance of the thermocline tank according to five design parameters and two dimensionless variables (external and internal shape factors) (Table 1), characterising the tank geometry and the filler particle size (Rebouillat et al., 2019). This dynamic model was validated using experimental data provided by the manufacturer (Rebouillat et al., 2019).

2.2.2 Life Cycle Assessment

LCA, a normalised method (ISO 14040 (International Organization for Standardization, 2020)), is carried out from "cradle-to-grave" to determine environmental impacts. The International reference Life Cycle Data system (ILCD) 2016 mid-point method is used to calculate the LCA indicators using EcoInvent v3.7.1 database (Ecoinvent, 2023) and OpenLCA v1.10 software (OpenLCA, 2023). The analysis of the reference TES is based on Lalau's works (Lalau et al., 2016, 2021). The TESM elaboration is based on (Lalau et al., 2021; Le Roux et al., 2022a). In order to fairly compare the environmental benefits of a system to the reference case, the same service is specified. The functional unit is defined as follows:

Provide a discharged thermal energy equal to that of the reference tank ($\boldsymbol{Q^*_{ds} = (Q_{ds})_{ES} = 1567\ kWh_{th}/cycle}$), during its lifespan (25 years) considering 2 cycles a day and 15 days off a year for maintenance.

Where Q^*_{ds} is the real discharge thermal energy computed by the physical model and $(Q_{ds})_{ES}$ the discharge thermal energy of the reference tank, Eco-Stock®.

Four environmental indicators, each representing a general impact category, are selected from previous LCA of CSP plants and TES (Burkhardt et al., 2011; Heath et al., 2010; Lalau et al., 2016):

- Cumulative Energy Demand (CED) in MJ_{eq}, related to energy impact category,
- Global Warming Potential (GWP) in $kgCO_{2\_eq}$, related to climate change impact category,
- Abiotic Depletion Potential of mineral, fossil and renewable resources (ADP) in $kg\ Sb_{eq}$, related to resource depletion impact category,
- Particulate matter (PM) in $kg\ PM2.5_{eq}$, related to human health impact category.

These four indicators are normalised according to European standards (ADEME, 2023; Institute for Environment and Sustainability (Joint Research Centre) et al., 2014). They are expressed in terms of European capita annual impact (ca.year). The sum of these normalised indicators defines the environmental optimisation criterion.

2.2.3 Life Cycle Cost Assessment

The economic model computes three indicators: Life Cycle Costs (LCC), Net Present Value (NPV) and LCOE. The first one represents the total amount of costs involved over the lifespan of the system (Azoumah, Tossa, and Dake 2020). The NPV is equal to the sum of the annual cash flows discounted to

the equivalent value at the start date of the project (Aussel et al., 2018). The LCOE is the selling price that cancels the NPV. In other words, it is the minimum energy selling price that ensures profitability. It can be expressed as a function of the LCC (Aussel et al., 2018) and the annual heat production H (in $kWh_{th}/year$):

$$LCOE = \frac{LCC}{US_f(N, i^*).H} \quad (4)$$

Where US_f is the Uniform Series factor. This factor adds up the annual revenues and discounts them over the lifespan (N years) of the system, using the discount rate and the inflation rate. The LCC includes capital (or investment), maintenance, operation, replacement and dismantling costs, and residual value. All costs are detailed in (Le Roux et al., 2022b). According to the functional unit previously defined for carrying out the LCA, the annual heat production is constant over the lifespan of the TES and worth 1 096 $MWh_{th}/year$. Thus, minimising the LCOE means maximising the NPV and minimising the LCC. Table 3 depicts the different economic parameters considered in this LCCA.

Table 3: Economic and energy parameters of the LCCA

Parameters		**Value**
Economic	Interest rate (% per year)	10
	Inflation rate (% per year)	3
	Real interest rate i^* (% per year)	6.8
	Uniform Series factor US_f	11.87
	Lifespan of the TES N (years)	25
Energy	Heat selling price P_{th} $(c€/kWh_{th})$	6.02 (France)

2.2.4 Optimisation algorithm

The optimal values of both shape factors are determined by minimising the objective function $\boldsymbol{f_{obj}}$, which includes the three criteria (η_{ex}, LCA and $LCOE$):

$$\begin{cases} f_{obj}(1) = 1 - \eta_{ex} = N_{ex} \\ f_{obj}(2) = LCA \\ f_{obj}(3) = LCOE \end{cases} \quad (5)$$

submitted to the constraint defined by the LCA. For each TESM, the optimisation problem then writes:

$$Min(\boldsymbol{f_{obj}}) \; with \; (Q_{ds})^* = (Q_{ds})_{ES} \quad (6)$$

Two determinist algorithms has been tested and compared: Particle Swarm Optimisation (PSO) and Genetic Algorithm (GA). For similar computation times, similar solutions were obtained for both algorithms. Since GA is well documented and widely used for energy systems, it was chosen to perform this multi-objective optimisation. Multi-criteria GA, based on the Non-Dominated Sorting Genetic Algorithm II (NSGA-II) method (Deb et al., 2002), available in Matlab® is used to solve this problem. Default parameters provided in Matlab® scripts are kept (Table 4). Varying the population size from 25 to 200 individuals, the number of generations from 100 to 1000 and the crossover and mutation probabilities of ± 0.1, similar results were obtained.

Table 4: Tuning parameters and settings for multi-criteria genetic algorithm

Parameters	Value
Population size	50
Number of generations	400
Initialisation mode	Random
Selection process	Tournament (size of 4)
Crossover probability	0.8
Mutation probability	0.2
Mutation distribution index	20

2.3 Multi-criteria optimisation: several filler materials case

The multi-objective optimisation consists of determining not only the best tank geometry, but also the best filler material to be implemented in the TES device among the seven TESM presented in Table 2. To select the best compromise solution, from the Pareto set obtained three successive steps are applied:

- **Step 1: Optimising the geometry for each single material,** as described in (Le Roux, et al. 2022b) This initial step provides seven Pareto sets.
- **Step 2: Building a single Pareto set encompassing the seven materials.** From the union of the seven Pareto sets obtained previously, only the non-dominated solutions are retained, defining a single Pareto set.
- **Step 3: Application of the decision-making method**. TOPSIS method with weights deduced from Shannon entropy is finally applied.

The step 3 combines two methods to determine the most desirable solution among those retained in the single Pareto set. "Technique for Order Preference by Similarity to Ideal Solution" (TOPSIS) (Hwang and Yoon, 1981) method is one of the simplest and of the most widely used methods in the energy sector. It is used for the selection step and ranks the different solutions from best to worst. The weighting step is derived from Shannon entropy (Shannon, 1948) to avoid subjective choices by the decision maker. Like TOPSIS, it is one of the most widely used methods and was therefore chosen for this study.

2.3.1 Step 1: Combination of the seven Pareto sets

Figure 1 shows the three-dimensional (3D) Pareto sets obtained by the multi-objective GA for bauxite (circles), alumina (plus signs), CFA (diamonds), CHCA (stars), cofalit (triangles), basalt (crosses) and quartzite (pentagons). The same marking code will be used in the following sections. Each Pareto set obtained with the multi-objective GA of Matlab® includes 18 optimal solutions among the initially generated population of 50 individuals.

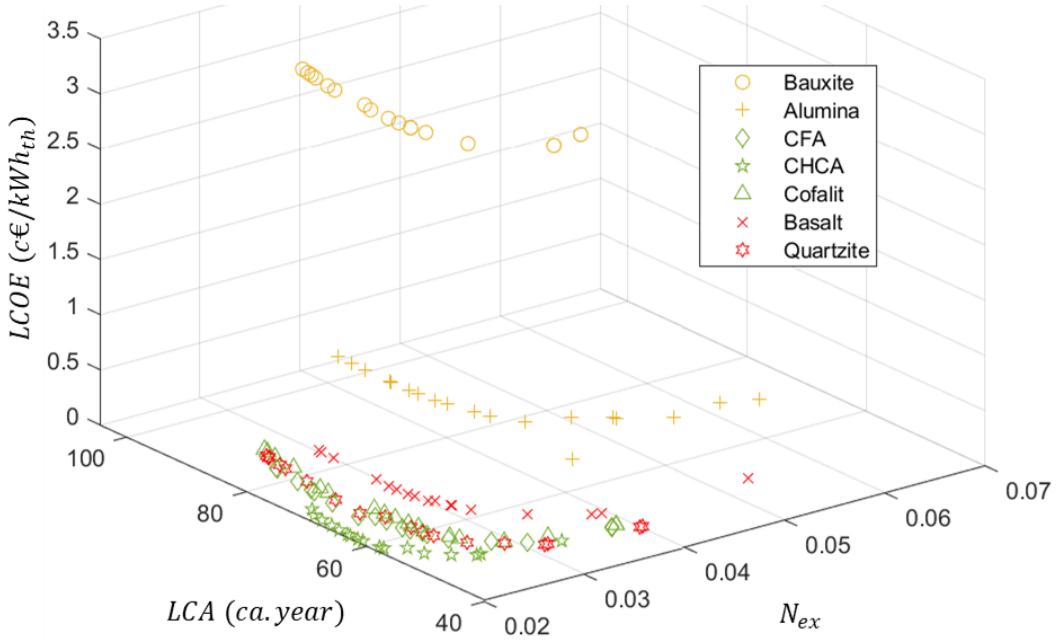

Figure 1: 3D Pareto sets of exergy/LCA/LCOE optimisations with genetic algorithm for seven fillers

Machined ceramics (bauxite and alumina) have the worst environmental and economic performance. Recycled ceramics and natural rocks have the smallest ecological footprint and the lowest LCOE. As for the exergy efficiency ($1 - N_{ex}$), it is similar for all the TESM (between 96.1 and 98.0%).

2.3.2 Step 2: Selection of non-dominated solutions

All the Pareto sets, bounded by the single-criterion optimisations, are combined and only the non-dominated solutions are shown in Figure 2. The resulting Pareto set contains 32 solutions. Only solutions with waste material or basalt appear. Therefore, machined ceramics are not interesting for industrial application in a thermocline TES. The ideal (I) and nadir (N) global solutions are marked in this figure.

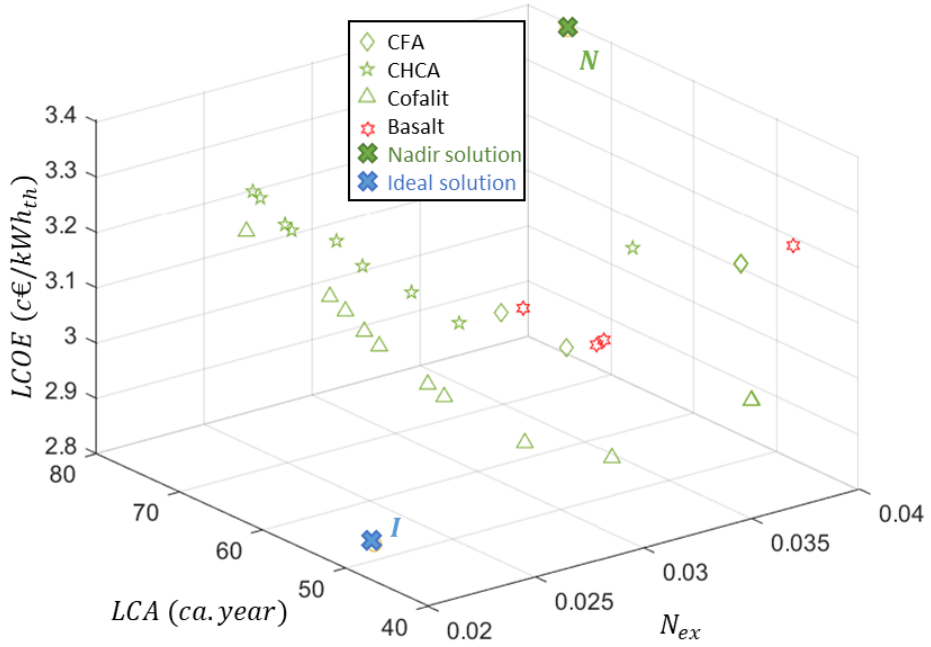

Figure 2: 3D Pareto set of non-dominated solutions for the seven filler material tested

2.3.3 Step 3: Decision-making method TOPSIS combined with Shannon entropy

The next steps are to determine the trade-off solution in the Pareto optimal set (Figure 2). The criteria are first linearly normalised (Shih et al., 2007) according to eq (A.3) :

$$\widetilde{N}_{ex,i} = \frac{N_{ex,i}}{\sum_{i=1}^{32} N_{ex,i}} = \frac{\eta_{ex,i}}{\sum_{i=1}^{32} \eta_{ex,i}}$$

$$\widetilde{LCA}_i = \frac{LCA_i}{\sum_{i=1}^{32} LCA_i} \tag{7}$$

$$\widetilde{LCOE}_i = \frac{LCOE_i}{\sum_{i=1}^{32} LCOE_i}$$

This normalisation method gives the three sets $\widetilde{N}_{ex,i}$, $\widetilde{LCA}_i$ and $\widetilde{LCOE}_i$ the properties of a probability ($\sum_{i=1}^{32} \widetilde{N}_{ex,i} = 1$, $\sum_{i=1}^{32} \widetilde{LCA}_i = 1$ and $\sum_{i=1}^{32} \widetilde{LCOE}_i = 1$) with the same mean value equal to 1/32.

Therefore, the Shannon entropy associated with each set of normalised criteria can be calculated (Appendix A.1), according to eqs (A.2) :

$$S_{ex} = -\frac{1}{\ln 32} \cdot \sum_{i=1}^{32} \widetilde{N}_{ex,i} \cdot \widetilde{N}_{ex,i} = 0.9937$$

$$S_{LCA} = -\frac{1}{\ln 32} \cdot \sum_{i=1}^{32} \widetilde{LCA}_i \cdot \ln \widetilde{LCA}_i = 0.9980 \tag{8}$$

$$S_{LCOE} = -\frac{1}{\ln 32} \cdot \sum_{i=1}^{32} \widetilde{LCOE}_i \cdot \ln \widetilde{LCOE}_i = 0.9997$$

The value of the Shannon entropy gives an account of the magnitude of the variation specific to each criterion. According to the definition (eq (8)), note that if all the values of a same criterion c_i are identical, the normalised values would be $\tilde{c}_i = 1/32$ for all solutions, which would lead to $S_c = 1$. This value corresponds to the maximum Shannon entropy, since it is relative to a uniform distribution (all solution c_i are equiprobable, their probability of occurrence being equal to 1/32). A value less than 1 means that the set of solutions is distributed over a certain interval, as shown in Figure 3.

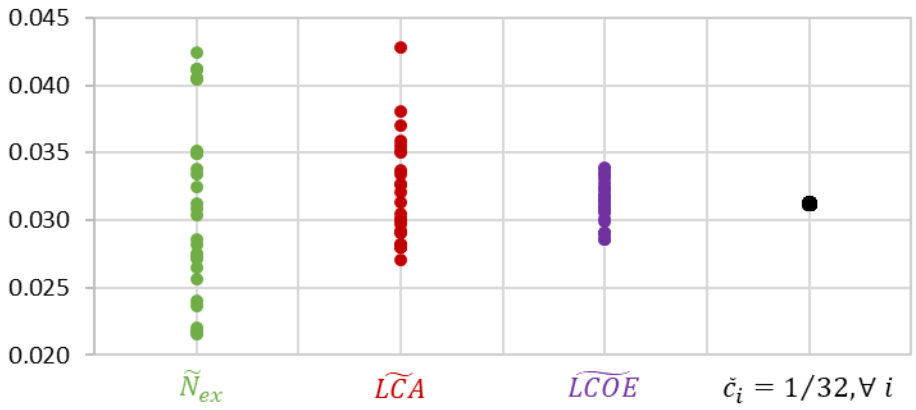

Figure 3: Optimal normalised non-dominated solutions compared to an equiprobable solution $\tilde{c}_i = constant$ (colour black for criterion c_i, green for exergy criterion, red for LCA criterion and purple for LCOE criterion)

An entropy value moving away from unity reflects a widening of the range of variation of the criterion. In this example, $S_{ex} < S_{LCA}. < S_{LCOE}$. The weights are then calculated according to the Shannon

entropy, giving preference to the most dispersed criterion. Consequently, the exergy weight should be higher than those of the LCA and LCOE criteria, as the following calculations show (eq (A.1)):

$$\omega_{ex} = \frac{1 - S_{ex}}{3 - S_{ex} - S_{LCA} - S_{LCOE}} = 0.733$$

$$\omega_{ACV} = \frac{1 - S_{ACV}}{3 - S_{ex} - S_{LCA} - S_{LCOE}} = 0.228 \quad (9)$$

$$\omega_{LCOE} = \frac{1 - S_{LCOE}}{3 - S_{ex} - S_{LCA} - S_{LCOE}} = 0.039$$

The weight resulting from the Shannon entropy give much less weight to the economic criterion. Indeed, the linearly normalised solutions are grouped around an average value (1/32 = 0.031 in Figure 3) for the LCOE. On the other hand, the exergy weight is greater than 0.7. The Shannon entropy gives less weight to criteria whose solutions are clustered around its mean value. In the case of virtual criterion c in Figure 3, the weight should be null as $S_c = 1$.

The weights resulting from the Shannon entropy are then applied to the normalised solutions:

$$\widehat{N}_{ex,i} = \omega_{ex} \cdot \widetilde{N}_{ex,i}, \qquad \widehat{LCA}_i = \omega_{ACV} \cdot \widetilde{LCA}_i, \qquad \widehat{LCOE}_i = \omega_{LCOE} \cdot \widetilde{LCOE}_i$$

and lead to the normalised and weighted Pareto front in Figure 4. The ideal I and nadir N solutions are respectively of coordinates $(\widehat{N}_{ex,min}, \widehat{LCA}_{min}, \widehat{LCOE}_{min})$ et $(\widehat{N}_{ex,max}, \widehat{LCA}_{max}, \widehat{LCOE}_{max})$. The TOPSIS method can now be applied. This method selects the optimal solution with the farthest distance from the nadir point N and the shortest distance from the ideal point I (Hwang and Yoon, 1981). The selected solution S is the one with the lowest ratio $\frac{SN}{SI+SN}$, I and N being respectively the ideal $(\widehat{N}_{ex,min}, \widehat{LCA}_{min}, \widehat{LCOE}_{min})$ and nadir solutions $(\widehat{N}_{ex,max}, \widehat{LCA}_{max}, \widehat{LCOE}_{max})$ (Figure 4). This solution as the best compromise is located on the left of the CHCA Pareto set ($\eta_{ex} = 0.980; LCA = 57.7\ ca.year; LCOE = 3.35\ c€/kWh_{th}$). This solution has one of the best exergy efficiency while the LCOE is one of the worst.

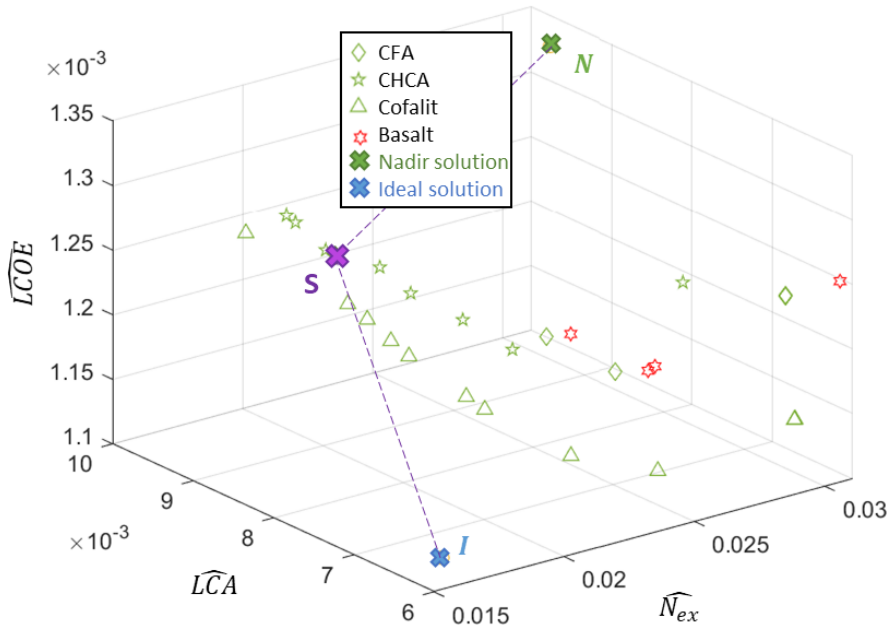

Figure 4: 3D normalised and weighted Pareto set of non-dominated solutions for the seven filler material tested and selection of the best compromise solution with TOPSIS

2.4 Overall structure of the multi-criteria optimisation of thermocline storage

The links between the physical, environmental and economic models and the decision-making methods are shown in Figure 5. The three models, the optimisation algorithm and the decision-making method TOPSIS have been detailed in (Le Roux et al., 2021; Le Roux et al., 2022b). To improve the selection of the best compromise solution, the Shannon entropy is combined with TOPSIS method. In TOPSIS method, a subjective weight is assigned to each criterion which is a problem. The Shannon entropy allows us to get rid of this subjective choice. For a HTF/TESM pair, Pareto set is obtained using the Matlab® multi-objective GA. The seven Pareto sets related to the seven HTF/TESM pairs studied are then combined. From this new set, a single Pareto set is constructed, consisting only of non-dominated solutions. TOPSIS combined with weight based on Shannon entropy (TOPSIS/Shannon) is then applied to select the best geometry for all the HTF/TESM pairs. The selected solution presents the best trade-off between geometry, particle size and filler material.

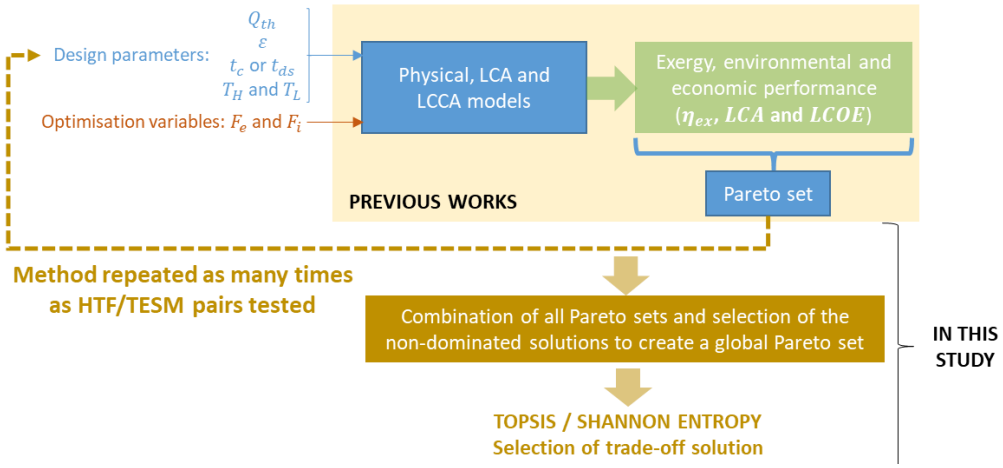

Figure 5: Overall structure of the multi-criteria optimisation with the inputs and outputs of each model

The objectives of this study are threefold. In a first step, seven filler materials are compared in the Eco-Stock® thermocline storage according to the three criteria: MC (bauxite, alumina), recycled ceramics (CFA, CHCA, cofalit) and natural rocks (basalt, quartzite) (Figure 1). In a second step, the seven Pareto fronts obtained are combined to form a single Pareto set by eliminating the dominated solutions (Figure 2). In this way, the geometry tank, the particle size and the filler material will be optimised at the same time. Finally, the Shannon entropy is used to improve the process of selecting the best trade-off solution. With this method the weight of each criterion is determined in an objective way (paragraph 2.3.3). Then, TOPSIS is applied with these weights (Figure 4).

3 Results and Discussions

This part was divided into two sections. Firstly, the performance and the geometry of the optimal solution selected in section 2.3 were studied. The optimisation variables of the non-dominated solutions selected from the seven Pareto sets obtained were investigated. Then, the performance of the optimised Eco-Stock® tank and the reference tank were compared.

3.1 Optimisation variables of the non-dominated solutions

As shown in section 2.3.3, MC and quartzite are rejected from the global Pareto set. MC are less attractive, particularly because of their high cost and high environmental impact. Quartzite has a low volumetric heat capacity ρc_p which does not allow it to be interesting in thermocline storage. The same ranking was done only on the thermophysical properties, environmental impact and cost of the fillers (Table 2) in Appendix A.2.

The non-dominated solutions shown in Figure 4 for the three optimisation criteria are presented in Figure 6 as a function of the two geometric optimisation variables (shape factors). The external shape factors (ratio diameter/length) ranged from 0.7 to 2.1, indicating an evolution of the storage geometry from tapered to square to stocky. The stocky tank shape was obtained when the exergy efficiency was high, while the tapered tank shape was preferred for low environmental impact and low costs, as explained in (Le Roux et al., 2021; Le Roux et al., 2022b). The internal shape factors ranged from 0.0023 to 0.0058. This indicated that the particle diameters remain small for each optimised solution, with less than 1 cm. It seems that the tapered the tank geometry, the larger the particle diameters. In addition, the non-dominated selected solutions with basalt had larger internal shape factors than those with CHCA, then cofalit and finally CFA. As a result, the smaller particle sizes were obtained for the solutions with CFA. The selected trade-off solution had an external shape factor of 1.11 and an internal shape factor of 0.003. This leads to a square shape with a small particle diameter.

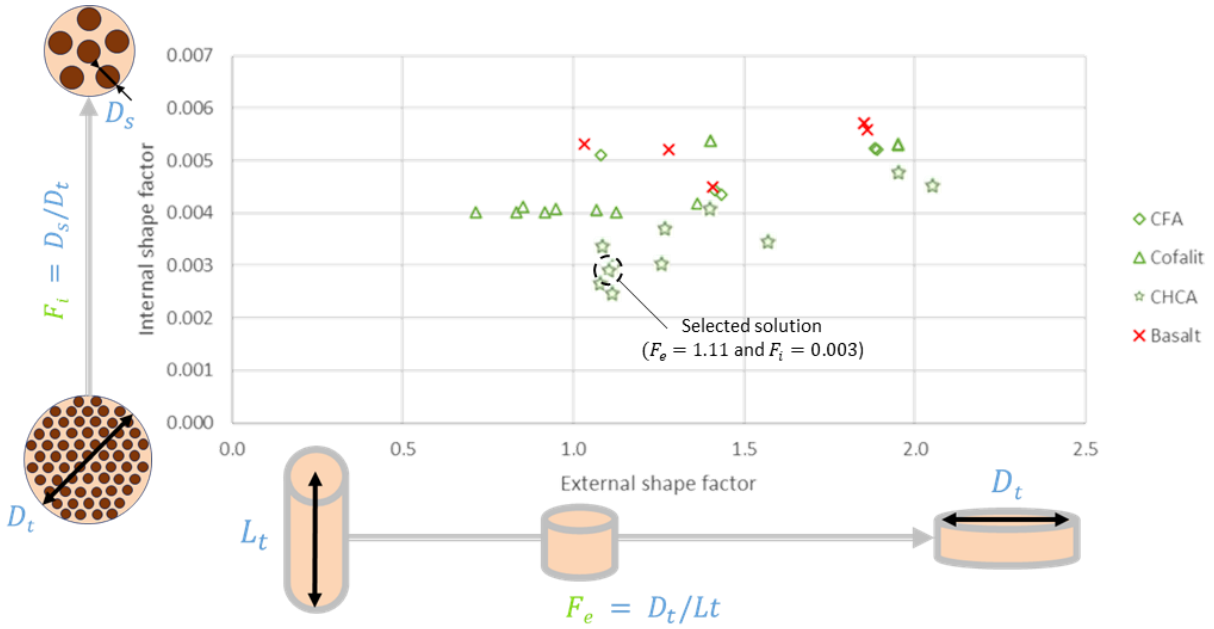

Figure 6: Shape factors of non-dominated solutions for the seven filler material tested

3.2 Comparison of the optimal solution and the Eco-Stock® reference tank

In this section, the selected solution was compared to the Eco-Stock® reference storage. The dimensions of the two TES are shown in Figure 7a. The green and blue colours refer respectively to the Eco-Stock® and the CHCA selected solution. Remind that both tanks provide the same thermal energy during one discharged step. The same colour codes will be used in the following section. The CHCA solution had a stocky shape whereas the Eco-Stock® was tapered. The particle size of the optimised tank was reduced compared to that of the reference tank. As for the storage volume, it was 25% higher for the optimised storage (9.3 vs 8.9 m^3). This is because the thermophysical properties of CHCA are poorer than those of bauxite, in particular the volumetric heat capacity ρc_p which is 26% lower (Table 2).

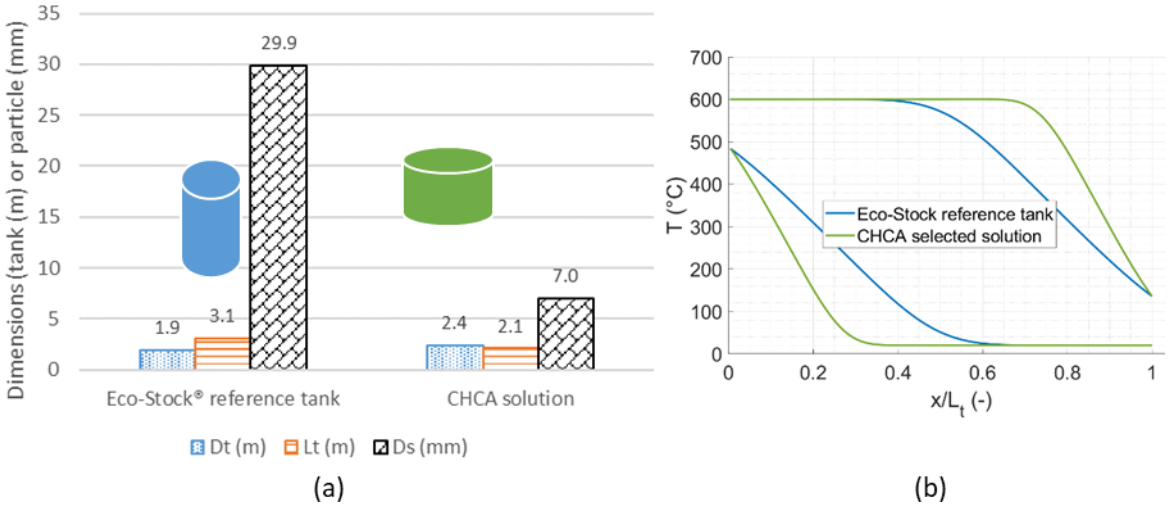

Figure 7: Comparison of the tank dimensions and particle size (a), temperature limit profiles of Eco-Stock® and CHCA selected solution (b)

The exergy, environmental and economic performance was then compared between these two storage systems. The temperature limit profiles of the periodic stationary behaviour are illustrated on Figure 7b as a function of their normalised length obtained for the reference tank and the CHCA solution. The temperature limit profiles of the optimised solution were steeper than those obtained for the Eco-Stock®. As a result, the stratification was better and the thermocline zone was thinner for the CHCA solution than for the reference tank. The boundaries of the temperature limit profiles represent the active zone of the storage. Due to better stratification, it was larger for the optimised solution (76.1%) and smaller for the Eco-Stock® (56.8%). The reference tank uses bauxite as filler material while a recycled ceramic (CHCA) is preferred for the optimised selected solution. Despite higher exergy utilisation rate, the volume of the optimised tank was greater than the reference TES for the same amount of delivered exergy (Figure 7a). Indeed, the product (ρc_p) is higher for bauxite (Table 2), indicating that bauxite can store more energy than CHCA.

The ecological footprint by life cycle phases and environmental indicators was compared for both configurations (reference and CHCA tanks) in Figure 8. The total environmental impact of the system was reduced by 13% for the optimised solution. The GWP, ADP and PM indicators were reduced respectively by 37, 10 and 25%. The use of recycled ceramic, such as CHCA, decreased the ecological impact of the elaboration of the filler (Table 2). The transport and end-of-life phases were also reduced by 20% thanks to the use of filler obtained from waste. Nevertheless, the environmental impact of these phases was very low. The use phase was 6 ca.year greater in the case of the optimised solution. This is due to the pressure drops, which were more than twice as high in this configuration due to the increased tank volume. As a result, the energy consumed by the fan was 119% higher. Despite the increase in the ecological impact of the use phase, the reduced impact of the TESM elaboration allowed the environmental footprint of the selected solution to be reduced by 9 ca.year compared to the Eco-Stock® reference.

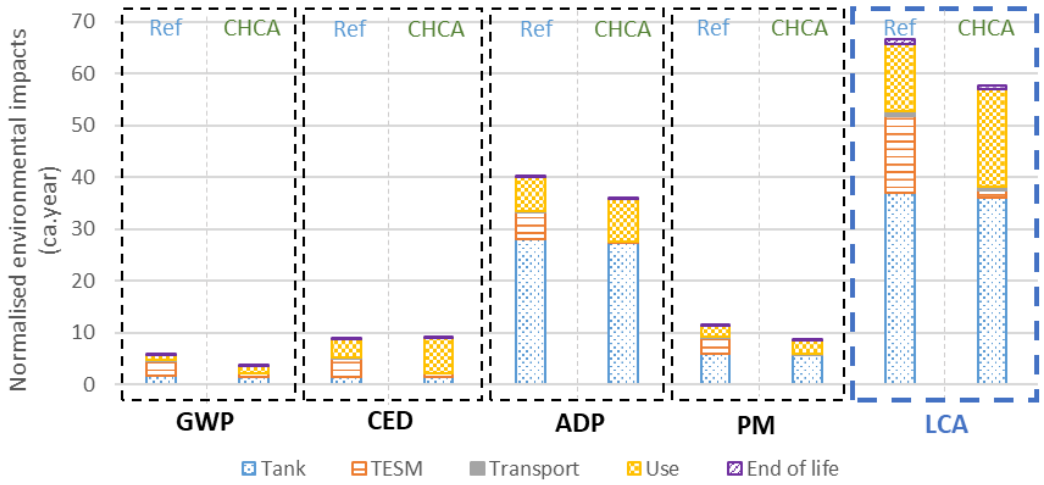

Figure 8: Comparison of LCA normalised indicators by phases of the life cycle for the Eco-Stock® and the CHCA selected solution

Figure 9 illustrates the three economic indicators for the reference tank and the CHCA selected solution. The economic performance of the CHCA solution was not as good as those of the Eco-Stock®. The small decrease in LCC and LCOE (1% reduction) resulted in a 5k€ reduction in NPV. The low cost of recycled ceramics allowed to limit the cost of TESM by 10k€ compared to machined ceramics such as bauxite. Despite this reduction, the increase in the pressure drop of the system led to an increase in the fan cost by 12k€. As a result, the LCOE of the CHCA selected solution reached 3.4 c€/kWh$_{th}$, which was 44% lower than the natural gas price in France.

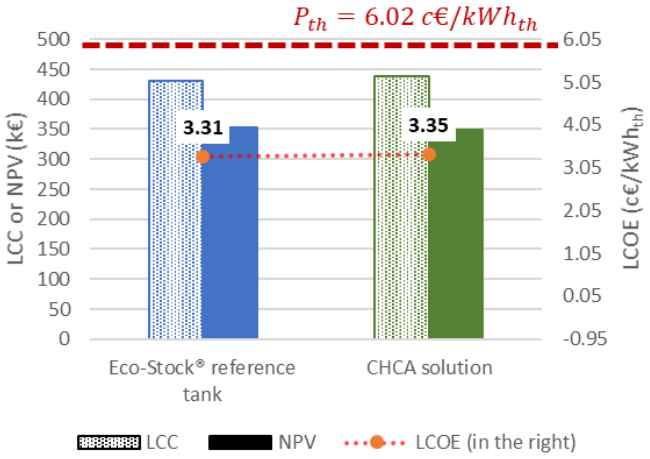

Figure 9: Comparison of economic indicators for the Eco-Stock® and the CHCA selected solution

The exergy and environmental performance was improved by using the optimised solution instead of the Eco-Stock®. Indeed, the exergy efficiency was slightly higher, with an increase of 2.5% compared to the reference tank. The environmental impacts were reduced by 13% due to the very low impact of CHCA compared to bauxite. The economic performance was slightly better with a 1% reduction. Despite the larger tank volume for the optimised solution, the TESM cost was negligible because CHCA are cheaper than bauxite. However, the CHCA solution used more pumping energy than the Eco-Stock®. Fan and operational costs were higher. These differences compensated each other, resulting in a close LCOE for the Eco-Stock® and the optimised solution: between 3.3 and 3.4 c€/kWh_{th}. Note that the Eco-Stock® was initially designed on an economic criterion. The main results of both tanks are given in Table 5.

Table 5: Dimensions and performance of the reference tank and the CHCA optimised solution selected by TOPSIS/Shannon

	Ref. tank	Optimised solution
HTF/TESM	**Air/Bauxite**	**Air/CHCA**
$D_t\ (m)$	1.92	2.36
$L_t\ (m)$	3.08	2.12
$D_s\ (mm)$	29.9	7.0
η_{ex}	95.6%	98.0%
$LCA\ tot.\ (ca.\ year)$	67	58
$LCOE\ (c€/kWh_{th})$	3.3	3.4

4 Conclusion

Multi-objective optimisation is performed on an industrial thermocline TES according to exergy, environmental and economic criteria. A one-dimensional two-phase model is applied to compute the exergy efficiency. The environmental footprint is determined by LCA and each TES system provide the same discharge exergy over its lifetime. The LCOE is calculated by LCCA. Seven different solid fillers are compared: machined ceramics (bauxite and alumina), recycled ceramics obtained from waste (CFA, CHCA and cofalit) and natural rocks (basalt and quartzite). This study seeks to find the optimal geometry of the thermocline tank, through two dimensionless variables, for a given HTF and filler material. The Matlab® multi-objective GA is used to solve the problem. A Pareto set of optimised solutions is obtained for each filler material tested. The seven 3D Pareto sets are combined to form a single Pareto set with non-dominated solutions. In order to select a compromise solution from this set, the TOPSIS method is combined with Shannon entropy to avoid subjective choice of the weights. The conclusions are summarised as follows:

1. The Shannon entropy favours the most dispersed criterion. Consequently, the impact of the exergy criterion is reinforced in this study with the highest weight associated with this criterion.
2. The application of the TOPSIS method leads to select the CHCA as the best compromise filler material tested in thermocline TES application. This result differs from the ranking of the same filler on their properties (Appendix A.2). As a result, it is important to consider the process in order to properly classify the filler materials.
3. This optimised solution has a square shape, whereas the Eco-Stock® is tapered. The particle diameter is significantly smaller for the CHCA selected solution, which leads to a better exergy efficiency. The storage volume of the optimised solution is a quarter larger due to the lower volumetric heat capacity of CHCA compared to bauxite. Despite this increase and so the energy consumed by the fan, the ecological footprint of the optimised storage is smaller than the Eco-Stock®. Indeed, the use of a material obtained from waste enables the ecological footprint of the TESM elaboration to be limited, which compensates the increased impact of the use phase of the system. As for the economic indicators, they are similar between both storages. The CHCA selected thermocline TES is very interesting from an exergy, environmental and economic point of view for heat storage. This confirms that materials derived from waste are very interesting to use as fillers for a heat storage application.

The methodology developed could be used by Eco-Tech Ceram to provide the best configuration of Eco-Stock® for the site operation. Future studies will focus on improving the existing methodology through an uncertainty study. In addition, the methodology will be implemented on other thermocline storage systems. A packed-bed storage system designed for the Andasol CSP plant in Spain (Fasquelle

et al., 2018) could be optimised in the same way, in order to apply the presented methodology to a solar application. In order to study the influence of operating temperatures, the storage of a tower CSP plant can also be optimised. The methodology could also be extended to an entire CSP plant, or to other energy applications.

Nomenclature

a	Specific area $(m^2 \cdot m^{-3})$
c	Heat capacity $(J \cdot kg^{-1} \cdot K^{-1})$
D	Diameter (m)
ex	Specific exergy $(J \cdot kg^{-1})$
F_e	External shape factor $(-)$
F_i	Internal shape factor $(-)$
H	Annual heat production $(kWh_{th}/year)$
h	Heat transfer coefficient $(J \cdot kg^{-1})$
i	Interest or discount rate $(\% \ / \ year)$
L	Length (m)
LCA	LCA criterion $(ca.year)$
LCC	Life Cycle Cost (€)
$LCOE$	Levelised Cost Of Energy criterion $(c€/kWh_{th})$
$\dot{m}$	Mass flow $(kg \cdot s^{-1})$
N	Lifetime of the system $(year)$
N_{ex}	Number of exergy destruction $(-)$
P	Energy price $(€/kWh_{th})$
Q	Energy capacity (J)
S	Shannon entropy $(-)$
T	Temperature (K)
t	Time (s)
u	Interstitial velocity of the fluid, i.e. Darcy velocity $(m \cdot s^{-1})$
U	Overall heat loss coefficient between the fluid and the outside $(W \cdot m^{-2} \cdot K^{-1})$
US_f	Uniform Series factor $(-)$

Greek symbols

Δ	Variation $(-)$
ε	Porosity $(-)$
η	Efficiency $(-)$
λ	Thermal conductivity $(W \cdot m^{-1} \cdot K^{-1})$
μ	Dynamic viscosity $(Pa \cdot s)$
ρ	Density $(kg \cdot m^{-3})$
τ_u	Utilisation rate $(-)$
ω	Weighting factor $(-)$

Subscripts and superscripts

*	Real
∞	Outdoor or free condition
$\frown$	Normalised and weighted criterion
$\sim$	Normalised criterion
c	Charge
ds	Discharge
ES	Eco-Stock®
eff	Effective
ex	Exergy
f	Fluid
fw	fluid/wall
H	Hot
L	Low
LCA	LCA
min	Minimum
max	Maximum
s	Solid
sf	solid/fluid
TESM	Filler material

t Tank

th Thermal

Abbreviations

ADP Abiotic Depletion Potential of mineral, fossil and renewable resources $(kg\ Sb_{eq})$

CED Cumulative Energy Demand (MJ_{eq})

CFA Ceramic from Fly Ashes

CSP Concentrating Solar Power

GA Genetic Algorithm

GWP Global Warming Potential $\left(kgCO_{2_{eq}}\right)$

HTF Heat Transfer Fluid

ILCD International Reference Life Cycle Data system

LCA Life Cycle Assessment

LCC Life Cycle Costs (€)

LCCA Life Cycle Cost Assessment

LCOE Levelised Cost Of Energy $(c€/kWh_{th})$

MC Machined Ceramic (bauxite)

NPV Net Present Value (€)

NSGA-II Non-Dominated Sorting Genetic Algorithm II

PM Particulate Matter $(kg\ PM2.5_{eq})$

PSO Particle Swarm Optimisation

TES Thermal Energy Storage

TESM Thermal Energy Storage Material

TOPSIS Technique for Order Preference by Similarity to Ideal Solution

A. Appendix

A.1. Shannon entropy

Shannon entropy quantifies the uncertainties of the information source, through a discrete probability distribution (Shannon 1948). The greater the entropy of an optimisation criterion (eq (A.2)), the lower its weight will be (eq (A.1)) (Jing et al. 2018). This weight ω_j is determined for each criterion j by:

$$\omega_j = \frac{1 - S_j}{o - \sum_{j=1}^{o} S_j}; \quad (j = 1, \dots, o); \quad with \sum_{j=1}^{o} \omega_j = 1 \tag{A.1}$$

where S_j is the Shannon entropy of criterion j. It is expressed as:

$$S_j = -\frac{1}{\ln n} \cdot \sum_{i=1}^{n} \tilde{m}_{ij} \cdot \ln \tilde{m}_{ij} \quad with\ 1 \le j \le o \tag{A.2}$$

$$\tilde{m}_{ij} = \frac{m_{ij}}{\sum_{i=1}^{n} m_{ij}} \tag{A.3}$$

A.2. Example: Selection of the best filler with TOPSIS/Shannon method

To illustrate the TOPSIS method combined with Shannon entropy based weights, the seven filler materials are ranked considering three criteria: effusivity, environmental footprint and cost. From the values presented in Table 6, linear normalization is applied (eq (A.3)) and lead to the evaluation matrix presented in Table 6.

Table 6: Evaluation matrix after normalisation (step 1)

	Step 1: linear Normalisation		
	$\widetilde{\epsilon_s}$	$\widetilde{LCA}$	$\widetilde{C_s}$
Bauxite	0.163	0.394	0.340
Alumina	0.190	0.403	0.604
CFA	0.131	0.052	0.011
CHCA	0.117	0.050	0.011
Cofalit	0.162	0.097	0.011
Quartzite	0.132	0.002	0.011
Basalt	0.105	0.001	0.011

Then, the normalised criteria are objectively weighted with the Shannon entropy. The entropy of each criterion is calculated according to eq (A.2) and the weights are determined (eq (A.1)). Table 7 shows the terms $\widetilde{\epsilon_s} \cdot \ln \widetilde{\epsilon_s}$, $\widetilde{LCA} \cdot \ln \widetilde{LCA}$ and $\widetilde{C_s} \cdot \ln \widetilde{C_s}$, the Shannon entropy and the weighting factor associated with each criterion.

Table 7: Shannon entropy of solutions and evaluation matrix after weighting (step 2)

	Shannon entropy			Step 2: Weighting		
	$\widetilde{\epsilon_s} \cdot \ln \widetilde{\epsilon_s}$	$\widetilde{LCA} \cdot \ln \widetilde{LCA}$	$\widetilde{C_s} \cdot \ln \widetilde{C_s}$	$\widehat{\epsilon_s}$	$\widehat{LCA}$	$\widehat{C_s}$
Bauxite	-2.96 10^{-1}	-3.67 10^{-1}	-3.67 10^{-1}	1.79 10^{-3}	1.53 10^{-1}	2.04 10^{-1}
Alumina	-3.15 10^{-1}	-3.66 10^{-1}	-3.05 10^{-1}	2.08 10^{-3}	1.57 10^{-1}	3.63 10^{-1}
CFA	-2.67 10^{-1}	-1.54 10^{-1}	-5.07 10^{-2}	1.44 10^{-3}	2.03 10^{-2}	6.80 10^{-3}
CHCA	-2.51 10^{-1}	-1.50 10^{-1}	-5.07 10^{-2}	1.28 10^{-3}	1.94 10^{-2}	6.80 10^{-3}
Cofalit	-2.95 10^{-1}	-2.26 10^{-1}	-5.07 10^{-2}	1.77 10^{-3}	3.76 10^{-2}	6.80 10^{-3}
Quartzite	-2.67 10^{-1}	-1.42 10^{-2}	-5.07 10^{-2}	1.44 10^{-3}	9.07 10^{-4}	6.80 10^{-3}

Basalt	-2.37 10^{-1}	-9.03 10^{-3}	-5.07 10^{-2}	1.15 10^{-3}	5.32 10^{-4}	6.80 10^{-3}
Shannon entropy	**9.90 10^{-1}**	**6.61 10^{-1}**	**4.75 10^{-1}**			
Weight	**1.09 10^{-2}**	**3.88 10^{-1}**	**6.01 10^{-1}**			

With the matrices normalised and weighted, the TOPSIS method can now be applied. The ideal and nadir solutions are determined. The Euclidian distances of each solution from the ideal SI and nadir SN solutions, as well as the ratio $R = \frac{SN}{SN+SI}$ between the distances are calculated. Finally, the solutions are ranked in ascending order according to the value of the ratio R. Table 8 shows the values of the Euclidian distances, the ratio of distances and the ranking assigned to the solutions. Quartzite is selected with this decision-making method as the best compromise filler material based on its properties. The resulting ranking was as follows: quartzite, basalt, CHCA, CFA, cofalit, bauxite and alumina. Consequently, the natural rocks or the recycled ceramics with the cheapest cost and the smallest ecological footprint seem to be best alternative than MC.

Table 8: Euclidian distances to ideal (SI, 2nd column) and nadir (SN, 3rd column) solutions, and ranking of solutions (4th and 5th columns)

Step 3: Decision-making method	SI	SN	R	Ranking
Bauxite	0.249	0.159	0.389	6
Alumina	0.389	0.001	0.002	7
CFA	0.020	0.381	0.951	4
CHCA	0.019	0.382	0.953	3
Cofalit	0.037	0.375	0.910	5
Quartzite	0.001	0.389	0.998	1
Basalt	0.001	0.389	0.998	2

Acknowledgements

This project has received funding from the Occitanie region under award number 19008845 ALDOCT 000791. The authors would like to thank Eco-Tech Ceram for sharing the data used in this study.

Bibliography

ADEME. 2018. *Excess Heat*. 2017th ed. Angers: ADEME.

ADEME. 2023 'base-empreinte.ademe'. *Base-Empreinte(R)*. Last access: 2 April 2023 (https://base-empreinte.ademe.fr/).

Aussel, D., P. Neveu, D. Tsuanyo, and Y. Azoumah. 2018. 'On the Equivalence and Comparison of Economic Criteria for Energy Projects: Application on PV/Diesel Hybrid System Optimal Design'. *Energy Conversion and Management* 163:493–506. doi: 10.1016/j.enconman.2017.12.050.

Azoumah, Yao K., Alain K. Tossa, and Rock A. Dake. 2020. 'Towards a Labelling for Green Energy Production Units: Case Study of off-Grid Solar PV Systems'. *Energy* 208:118149. doi: 10.1016/j.energy.2020.118149.

Brans, J. P., and Ph Vincke. 1984. 'Preference Ranking Organisation Method for Enrichment Evaluations (The PROMETHEE Method for Multiple Criteria Decision Making)'. *Centrum Voor Statistiek En Operationeel Onderzoek, Vrije Universiteit, Brussel*.

Brosseau, Doug, John W. Kelton, Daniel Ray, Mike Edgar, Kye Chisman, and Blaine Emms. 2005. 'Testing of Thermocline Filler Materials and Molten-Salt Heat Transfer Fluids for Thermal Energy Storage Systems in Parabolic Trough Power Plants'. *Journal of Solar Energy Engineering* 127(1):109–16. doi: 10.1115/1.1824107.

Burkhardt, John J., Garvin A. Heath, and Craig S. Turchi. 2011. 'Life Cycle Assessment of a Parabolic Trough Concentrating Solar Power Plant and the Impacts of Key Design Alternatives'. *Environmental Science & Technology* 45(6):2457–64. doi: 10.1021/es1033266.

Dai, Baomin, Yu Cao, Shengchun Liu, Yalan Ji, Zhili Sun, Tianyahui Xu, Peng Zhang, and Victor Nian. 2022. 'Annual Energetic Evaluation of Multi-Stage Dedicated Mechanical Subcooling Carbon Dioxide Supermarket Refrigeration System in Different Climate Regions of China Using Genetic Algorithm'. *Journal of Cleaner Production* 333:130119. doi: 10.1016/j.jclepro.2021.130119.

Deb, K., A. Pratap, S. Agarwal, and T. Meyarivan. 2002. 'A Fast and Elitist Multiobjective Genetic Algorithm: NSGA-II'. *IEEE Transactions on Evolutionary Computation* 6(2):182–97. doi: 10.1109/4235.996017.

Deng, Hepu, Chung-Hsing Yeh, and Robert J. Willis. 2000. 'Inter-Company Comparison Using Modified TOPSIS with Objective Weights'. *Computers & Operations Research* 27(10):963–73. doi: 10.1016/S0305-0548(99)00069-6.

Diakoulaki, D., G. Mavrotas, and L. Papayannakis. 1995. 'Determining Objective Weights in Multiple Criteria Problems: The Critic Method'. *Computers & Operations Research* 22(7):763–70. doi: 10.1016/0305-0548(94)00059-H.

Ding, Pan, Ke Zhang, Zhihua Yuan, Zhenguo Wang, Dongliang Li, Tiancai Chen, Junjuan Shang, and Rahim Shofahaei. 2021. 'Multi-Objective Optimization and Exergoeconomic Analysis of Geothermal-Based Electricity and Cooling System Using Zeotropic Mixtures as the Working Fluid'. *Journal of Cleaner Production* 294:126237. doi: 10.1016/j.jclepro.2021.126237.

Ecoinvent. 2023 'Ecoinvent.Org'. *Ecoinvent*. Last access: 2 April 2023 (https://www.ecoinvent.org/).

Eco-Tech Ceram. 2023 'ecotechceram.com'. *Eco-Tech Ceram*. Last access: 2 April 2023 (https://www.ecotechceram.com/).

Fasquelle, T., Q. Falcoz, P. Neveu, and J. F. Hoffmann. 2018. 'Numerical Simulation of a 50 MWe Parabolic Trough Power Plant Integrating a Thermocline Storage Tank'. *Energy Conversion and Management* 172:9–20. doi: 10.1016/j.enconman.2018.07.006.

Forman, Clemens, Ibrahim Kolawole Muritala, Robert Pardemann, and Bernd Meyer. 2016. 'Estimating the Global Waste Heat Potential'. *Renewable and Sustainable Energy Reviews* 57:1568–79. doi: 10.1016/j.rser.2015.12.192.

Heath, Garvin, Craig Turchi, Terese Decker, John Burkhardt, and Chuck Kutscher. 2010. 'Life Cycle Assessment of Thermal Energy Storage: Two-Tank Indirect and Thermocline'. Pp. 689–90 in *ASME 2009 3rd International Conference on Energy Sustainability, Volume 2*. San Francisco, California, USA: American Society of Mechanical Engineers Digital Collection.

Huang, Jingwen. 2008. 'Combining Entropy Weight and TOPSIS Method for Information System Selection'. Pp. 1281–84 in *2008 IEEE Conference on Cybernetics and Intelligent Systems*.

Hwang, Ching-Lai, and Kwangsun Yoon. 1981. *Multiple Attribute Decision Making: Methods and Applications A State-of-the-Art Survey*. Berlin Heidelberg: Springer.

Institute for Environment and Sustainability (Joint Research Centre), Lucia Mancini, Erwin M. Schau, Serenella Sala, Rana Pant, Simone Manfredi, and Lorenzo Benini. 2014. *Normalisation Method and Data for Environmental Footprints*. Luxembourg: Publications Office of the European Union.

International Organization for Standardization. 2020. *ISO 14040 - Environmental Management — Life Cycle Assessment — Principles and Framework*. BS EN ISO 14040:2006+A1:2020. British Standard Institution.

Jafaryeganeh, H., M. Ventura, and C. Guedes Soares. 2020. 'Application of Multi-Criteria Decision Making Methods for Selection of Ship Internal Layout Design from a Pareto Optimal Set'. *Ocean Engineering* 202:107151. doi: 10.1016/j.oceaneng.2020.107151.

Jing, Rui, Xingyi Zhu, Zhiyi Zhu, Wei Wang, Chao Meng, Nilay Shah, Ning Li, and Yingru Zhao. 2018. 'A Multi-Objective Optimization and Multi-Criteria Evaluation Integrated Framework for Distributed Energy System Optimal Planning'. *Energy Conversion and Management* 166:445–62. doi: 10.1016/j.enconman.2018.04.054.

Johnson, Ilona, William T. Choate, and Amber Davidson. 2008. *Waste Heat Recovery. Technology and Opportunities in U.S. Industry*. BCS, Inc., Laurel, MD (United States). doi: 10.2172/1218716.

Keshavarz-Ghorabaee, Mehdi, Maghsoud Amiri, Edmundas Kazimieras Zavadskas, Zenonas Turskis, and Jurgita Antucheviciene. 2018. 'Simultaneous Evaluation of Criteria and Alternatives (SECA) for Multi-Criteria Decision-Making'. *Informatica* 29(2):265–80.

Kim, Seongjun, and Sung-Ah Kim. 2021. 'Design Optimization of Noise Barrier Tunnels through Component Reuse: Minimization of Costs and CO2 Emissions Using Multi-Objective Genetic Algorithm'. *Journal of Cleaner Production* 298:126697. doi: 10.1016/j.jclepro.2021.126697.

Lalau, Y., X. Py, A. Meffre, and R. Olives. 2016. 'Comparative LCA Between Current and Alternative Waste-Based TES for CSP'. *Waste and Biomass Valorization* 7(6):1509–19. doi: 10.1007/s12649-016-9549-6.

Lalau, Yasmine, Ibrahim Al Asmi, Régis Olives, Guilhem Dejean, Antoine Meffre, and Xavier Py. 2021. 'Energy Analysis and Life Cycle Assessment of a Thermal Energy Storage Unit Involving Conventional or Recycled Storage Materials and Devoted to Industrial

Waste Heat Valorisation'. *Journal of Cleaner Production* 129950. doi: 10.1016/j.jclepro.2021.129950.

Le Roux, D., Y. Lalau, B. Rebouillat, P. Neveu, and R. Olivès. 2021. 'Thermocline Thermal Energy Storage Optimisation Combining Exergy and Life Cycle Assessment'. *Energy Conversion and Management* 248:114787. doi: 10.1016/j.enconman.2021.114787.

Le Roux, D., P. Neveu, and R. Olivès. 2022a. 'Multi-Criteria Optimisation of an Industrial Thermocline Thermal Energy Storage'. Pp. 147–58 in *Proceedings of ECOS 2022*. Copenhaguen.

Le Roux, D., R. Olivès, and P. Neveu. 2022b. 'Geometry Optimisation of an Industrial Thermocline Thermal Energy Storage Combining Exergy, Life Cycle Assessment and Life Cycle Cost Analysis'. *Journal of Energy Storage* 55:105776. doi: 10.1016/j.est.2022.105776.

Li, Peiyue, Hui Qian, Jianhua Wu, and Jie Chen. 2013. 'Sensitivity Analysis of TOPSIS Method in Water Quality Assessment: I. Sensitivity to the Parameter Weights'. *Environmental Monitoring and Assessment* 185(3):2453–61. doi: 10.1007/s10661-012-2723-9.

Liu, Hu-Chen, Xu-Qi Chen, Chun-Yan Duan, and Ying-Ming Wang. 2019a. 'Failure Mode and Effect Analysis Using Multi-Criteria Decision Making Methods: A Systematic Literature Review'. *Computers & Industrial Engineering* 135:881–97. doi: 10.1016/j.cie.2019.06.055.

Liu, Xianfeng, Xinxing Zhou, Bangzhu Zhu, Kaijian He, and Ping Wang. 2019b. 'Measuring the Maturity of Carbon Market in China: An Entropy-Based TOPSIS Approach'. *Journal of Cleaner Production* 229:94–103. doi: 10.1016/j.jclepro.2019.04.380.

Luo, Zhengyi, Sheng Yang, Nan Xie, Weiwei Xie, Jiaxing Liu, Yawovi Souley Agbodjan, and Zhiqiang Liu. 2019. 'Multi-Objective Capacity Optimization of a Distributed Energy System Considering Economy, Environment and Energy'. *Energy Conversion and Management* 200:112081. doi: 10.1016/j.enconman.2019.112081.

Maystre, Lucien Yves, Jacques Pictet, and Jean Simos. 1994. *Méthodes multicritères ELECTRE: description, conseils pratiques et cas d'application à la gestion environnementale*. première. Lausanne: PPUR presses polytechniques.

Olson, D. L. 2004. 'Comparison of Weights in TOPSIS Models'. *Mathematical and Computer Modelling* 40(7):721–27. doi: 10.1016/j.mcm.2004.10.003.

OpenLCA. 2023 'OpenLCA.Org'. *OpenLCA*. Last access: 2 April 2023 (https://www.openlca.org/).

Opricovic, S. 1998. 'Multicriteria Optimization in Civil Engineering'. Faculty of Civil Engineering, Belgarde.

Panayiotou, Gregoris P., Giuseppe Bianchi, Giorgos Georgiou, Lazaros Aresti, Maria Argyrou, Rafaela Agathokleous, Konstantinos M. Tsamos, Savvas A. Tassou, Georgios Florides, Soteris Kalogirou, and Paul Christodoulides. 2017. 'Preliminary Assessment of Waste Heat Potential in Major European Industries'. *Energy Procedia* 123:335–45. doi: 10.1016/j.egypro.2017.07.263.

Plisson, Pauline, Sébastien Devroe, Aurélie Gonzalez, Aliénor Guiard, Guillaume Denis, and Claire Mathieu. 2017. *Waste Heat Recovery: Technologically and Economically Viable Solutions for Industrial Businesses - A White Book on Industrial Waste Heat Recovery*. Fives group.

Rahman, Md Mustafizur, Abayomi Olufemi Oni, Eskinder Gemechu, and Amit Kumar. 2020. 'Assessment of Energy Storage Technologies: A Review'. *Energy Conversion and Management* 223:113295. doi: 10.1016/j.enconman.2020.113295.

Rao, R. V., and B. K. Patel. 2010. 'A Subjective and Objective Integrated Multiple Attribute Decision Making Method for Material Selection'. *Materials & Design* 31(10):4738–47. doi: 10.1016/j.matdes.2010.05.014.

Rebouillat, Baptiste, Quentin Falcoz, and Pierre Neveu. 2019. '2nd Law Analysis of Thermocline – Heat Storage System'. Pp. 3065–76 in *ECOS 2019*. Wrocław, Poland: Institute of Thermal Technology - Silesian University of Technology.

Saaty, T. L. 1980. 'The Analytical Hierarchy Process'. Mc Graw-Hill, New York.

Saeidi, Parvaneh, Abbas Mardani, Arunodaya Raj Mishra, Viviana Elizabeth Cajas Cajas, and Mercedes Galarraga Carvajal. 2022. 'Evaluate Sustainable Human Resource Management in the Manufacturing Companies Using an Extended Pythagorean Fuzzy SWARA-TOPSIS Method'. *Journal of Cleaner Production* 370:133380. doi: 10.1016/j.jclepro.2022.133380.

dos Santos, Bruno Miranda, Leoni Pentiado Godoy, and Lucila M. S. Campos. 2019. 'Performance Evaluation of Green Suppliers Using Entropy-TOPSIS-F'. *Journal of Cleaner Production* 207:498–509. doi: 10.1016/j.jclepro.2018.09.235.

Shannon, C. E. 1948. 'A Mathematical Theory of Communication'. *The Bell System Technical Journal* 27(3):379–423. doi: 10.1002/j.1538-7305.1948.tb01338.x.

Shih, Hsu-Shih, Huan-Jyh Shyur, and E. Stanley Lee. 2007. 'An Extension of TOPSIS for Group Decision Making'. *Mathematical and Computer Modelling* 45(7):801–13. doi: 10.1016/j.mcm.2006.03.023.

Siksnelyte, Indre, Edmundas Kazimieras Zavadskas, Dalia Streimikiene, and Deepak Sharma. 2018. 'An Overview of Multi-Criteria Decision-Making Methods in Dealing with Sustainable Energy Development Issues'. *Energies* 11(10):2754. doi: 10.3390/en11102754.

Solymosi, Tamás, and József Dombi. 1986. 'A Method for Determining the Weights of Criteria: The Centralized Weights'. *European Journal of Operational Research* 26(1):35–41. doi: 10.1016/0377-2217(86)90157-8.

Srinivasan, V., and Allan D. Shocker. 1973. 'Linear Programming Techniques for Multidimensional Analysis of Preferences'. *Psychometrika* 38(3):337–69. doi: 10.1007/BF02291658.

Touzo, Aubin, Régis Olives, Guilhem Dejean, Doan Pham Minh, Mouna El Hafi, Jean-François Hoffmann, and Xavier Py. 2020. 'Experimental and Numerical Analysis of a Packed-Bed Thermal Energy Storage System Designed to Recover High Temperature Waste

Heat: An Industrial Scale Up'. *Journal of Energy Storage* 32:101894. doi: 10.1016/j.est.2020.101894.

Tsuanyo, David, Yao Azoumah, Didier Aussel, and Pierre Neveu. 2015. 'Modeling and Optimization of Batteryless Hybrid PV (Photovoltaic)/Diesel Systems for off-Grid Applications'. *Energy* 86:152–63. doi: 10.1016/j.energy.2015.03.128.

Tu, Yan, Huayi Wang, Xiaoyang Zhou, Wenjing Shen, and Benjamin Lev. 2021. 'Comprehensive Evaluation of Security, Equity, and Efficiency on Regional Water Resources Coordination Using a Hybrid Multi-Criteria Decision-Making Method with Different Hesitant Fuzzy Linguistic Term Sets'. *Journal of Cleaner Production* 310:127447. doi: 10.1016/j.jclepro.2021.127447.

Wang, Zhanzhou, Lihua Cao, and Heyong Si. 2021. 'An Improved Genetic Algorithm for Determining the Optimal Operation Strategy of Thermal Energy Storage Tank in Combined Heat and Power Units'. *Journal of Energy Storage* 43:103313. doi: 10.1016/j.est.2021.103313.

Wolff, Sebastian, Moritz Seidenfus, Matthias Brönner, and Markus Lienkamp. 2021. 'Multi-Disciplinary Design Optimization of Life Cycle Eco-Efficiency for Heavy-Duty Vehicles Using a Genetic Algorithm'. *Journal of Cleaner Production* 318:128505. doi: 10.1016/j.jclepro.2021.128505.

Zadeh, L. A. 1965. 'Fuzzy Sets'. *Information and Control* 8(3):338–53. doi: 10.1016/S0019-9958(65)90241-X.

Zadeh, L. A. 1968. 'Fuzzy Algorithm'. *Information and Control* 12:338–53.

Zhang, Mingyang, and Jihong Yan. 2021. 'A Data-Driven Method for Optimizing the Energy Consumption of Industrial Robots'. *Journal of Cleaner Production* 285:124862. doi: 10.1016/j.jclepro.2020.124862.

Zhao, Defu, Cunbin Li, Qiqing Wang, and Jiahai Yuan. 2020. 'Comprehensive Evaluation of National Electric Power Development Based on Cloud Model and Entropy Method and TOPSIS: A Case Study in 11 Countries'. *Journal of Cleaner Production* 277:123190. doi: 10.1016/j.jclepro.2020.123190.